

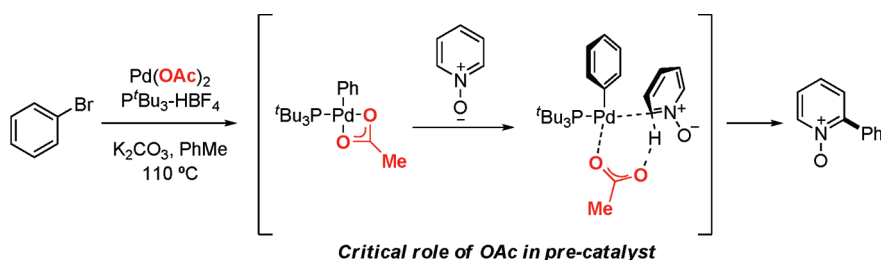
Mechanistic Analysis of Azine *N*-Oxide Direct Arylation: Evidence for a Critical Role of Acetate in the Pd(OAc)₂ Precatalyst

Ho-Yan Sun, Serge I. Gorelsky, David R. Stuart, Louis-Charles Campeau,* and
Keith Fagnou[†]

Center for Catalysis Research and Innovation, Department of Chemistry, University of Ottawa 10 Marie Curie,
Ottawa, Ontario, Canada K1N 6N5. [†]Deceased November 11, 2009

louis-charles_campeau@merck.com

Received September 15, 2010



Detailed mechanistic studies on the palladium-catalyzed direct arylation of pyridine *N*-oxides are presented. The order of each reaction component is determined to provide a general mechanistic picture. The C–H bond cleaving step is examined in further detail through computational studies, and the calculated results are in support of an inner-sphere concerted metalation–deprotonation (CMD) pathway. Competition experiments were conducted with *N*-oxides of varying electronic characters, and results revealed an enhancement of rate when using a more electron-deficient species, which is in support of a CMD transition state. The effect of base on reaction rate was also examined and it was found that a carboxylate base was required for the reaction to proceed. This led to the conclusion that Pd(OAc)₂ plays a pivotal role in the reaction mechanism as more than merely a precatalyst, but also as a source of acetate base required for the C–H bond cleavage step.

Introduction

The formation of carbon–carbon bonds via direct arylation has undergone significant advances in recent years with efforts focused toward expanding substrate scope and novel catalyst development.¹ In light of these studies, direct arylation of aryl halides has become an attractive alternative to the use of stoichiometric organometallic reagents in the preparation of biaryl compounds. Our group and others have been successful in developing a range of methods allowing

for the coupling of electron-rich,² -neutral,³ and -poor⁴ arenes (Scheme 1). While these reactions are synthetically useful, the development of novel catalysts which show increased reactivity at lower temperatures and catalyst loadings still remains a challenge. A better mechanistic understanding of direct arylation is crucial to the development of new catalysts as there are relatively few of these studies published to date.^{2,5–7} Such studies would be useful when developing new reactions, allowing for improvements to be made to existing reaction conditions and in the development of specially

(1) For comprehensive reviews on direct arylations, see: (a) Ackermann, L.; Vicente, R.; Kapdi, A. R. *Angew. Chem., Int. Ed.* **2009**, *48*, 9792. (b) Campeau, L.-C.; Stuart, D. R.; Fagnou, K. *Aldrichim. Acta* **2007**, *40*, 35. (c) Alberico, D.; Scott, M. E.; Lautens, M. *Chem. Rev.* **2007**, *107*, 174. (d) *Modern Arylation Methods*; Ackermann, L., Ed.; Wiley-VCH: Weinheim, Germany, 2009.

(2) (a) Park, C.-H.; Ryabova, V.; Seregin, I. V.; Sromek, A. W.; Gevorgyan, V. *Org. Lett.* **2004**, *6*, 1159. (b) Lane, B. S.; Brown, M. A.; Sames, D. *J. Am. Chem. Soc.* **2005**, *127*, 8050. (c) Chuprakov, S.; Chernyak, N.; Dudnik, A. S.; Gevorgyan, V. *Org. Lett.* **2007**, *9*, 2333.

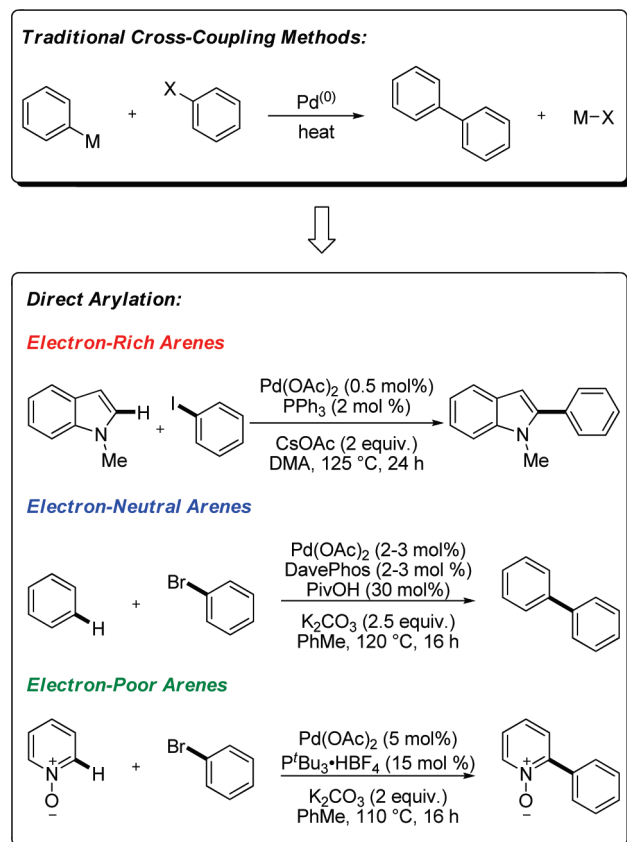
(3) Lafrance, M.; Rowley, C. N.; Woo, T. K.; Fagnou, K. *J. Am. Chem. Soc.* **2006**, *128*, 8754.

(4) (a) Campeau, L.-C.; Rousseaux, S.; Fagnou, K. *J. Am. Chem. Soc.* **2005**, *127*, 18021. (b) Campeau, L.-C.; Stuart, D. R.; Leclerc, J.-P.; Bertrand-Laperle, M.; Villemure, E.; Sun, H.-Y.; Lasserre, S.; Guimond, N.; Lecavallier, M.; Fagnou, K. *J. Am. Chem. Soc.* **2009**, *131*, 3291.

(5) (a) Garcia-Cuadrado, D.; Braga, A. A. C.; Maseras, F.; Echavarren, A. M. *J. Am. Chem. Soc.* **2006**, *128*, 1066. (b) Garcia-Cuadrado, D.; de Mendoza, P.; Braga, A. A. C.; Maseras, F.; Echavarren, A. M. *J. Am. Chem. Soc.* **2007**, *129*, 6880.

(6) (a) Pivsa-Art, S.; Satoh, T.; Kawamura, Y.; Miura, M.; Nomura, B. *Bull. Chem. Soc. Jpn.* **1998**, *71*, 467. (b) Yanagisawa, S.; Sudo, T.; Noyori, R.; Itami, K. *J. Am. Chem. Soc.* **2006**, *128*, 11748.

SCHEME 1. The Evolution of Cross-Coupling Methods



designed catalysts to reveal the necessary reactivity for an even broader range of direct C–H bond transformations in organic synthesis.

Of the studies directed toward elucidating the mechanism of direct arylation, computational studies have been prominently featured while little experimental evidence in support of the various proposals has been brought forth. Electrophilic, nucleophilic, and electron-neutral palladium aryl species have all been suggested to interact with aromatic substrates of varying electronic characters. Moreover, few if any of these studies deal with the relationship between precatalyst and active catalyst. Studies of this kind have been crucial to the development of very active catalysts in other palladium-catalyzed processes. In our previous report of this chemistry, we related the preliminary findings of experimental results aimed at elucidating the mechanism of the C–H bond cleaving process.⁴ Herein we describe a detailed investigation of the possible modes of C–H bond cleavage in the direct arylation of pyridine *N*-oxides. Coupled with detailed kinetic studies and other key experimental evidence, DFT calculations were performed for the four most commonly proposed mechanisms for direct arylation. Stoichiometric studies have also been used to elucidate the role of base in this transformation and have led to an unexpected and critical role of the acetate

ligand on the precatalyst in the active catalyst formed in direct arylation. These studies have led to the advancement of a catalytic cycle for direct arylation of pyridine *N*-oxide.

The most discussed mechanisms of direct arylation are the carbopalladation or Heck-type pathway,⁷ the oxidative insertion pathway,^{8–10} the electrophilic palladation or electrophilic aromatic substitution ($S_{\text{E}}\text{Ar}$) pathway,^{2,6} and the concerted metalation–deprotonation (CMD) pathway.^{3,5,11} (Scheme 2).

The Heck-type pathway (path A) is characterized by *syn*-addition of a palladium–carbon bond across a double bond of the aromatic coupling partner. While *anti*- β -hydride elimination is a high-energy process, the formation of a π -allyl species is often proposed, which could then isomerize to allow for a lower energy *syn*- β -hydride elimination.^{7a}

Less described in the literature is the oxidative addition of a Pd^{II} species to a Pd^{IV} species through an insertion into a C–H bond of an aromatic coupling partner (path B). A double reductive elimination would then afford the biaryl product as well as regenerate the catalytically active Pd^{II} species.

To date, the most commonly suggested hypothesis for the mechanism of direct arylation is electrophilic palladation (path C). Originally proposed for the arylation of electron-rich heteroarenes, this has since been referenced numerous times for other direct arylation reactions.^{2,6,12} An electrophilic palladation or electrophilic aromatic substitution ($S_{\text{E}}\text{Ar}$) type process would involve a rate-determining nucleophilic attack by the arene on an electrophilic Pd^{II} -aryl species followed by rapid deprotonation of the resulting Wheland intermediate. Subsequent reductive elimination of the biaryl from Pd^{II} would form the desired carbon–carbon bond as well as regenerate the active catalyst.

Our group and others have found computationally that for simple or electron-deficient aromatics, a CMD pathway (path D) is the lowest energy process, which was consistent with experimental observations.^{3,4,13,14} In a CMD pathway, the Pd–C bond formation occurs concurrently with the cleavage of the C–H bond of the arene to afford a Pd^{II} diaryl species. This is then followed by reductive elimination of the biaryl product, regenerating the active catalyst. While convincing computational evidence has been reported,¹¹ there have been very few reports of in-depth experimental support for a CMD mechanism.

Results and Discussion

1. Kinetics. The generally accepted mechanism for palladium-catalyzed direct arylation of aryl halides and simple arenes is shown in Scheme 3. The active Pd^{II} catalyst undergoes oxidative insertion into the aryl halide, followed by C–H bond cleavage of the simple arene. Reductive elimination provides the

(7) (a) McClure, M. S.; Glover, B.; McSorley, E.; Millar, A.; Osterhout, M. H.; Roschinger, F. *Org. Lett.* **2001**, *3*, 1677. (b) Glover, B.; Harvey, K. A.; Liu, B.; Sharp, M. J.; Tymoschenko, M. F. *Org. Lett.* **2003**, *5*, 301. (c) Li, W.; Nelson, D. P.; Jensen, M. S.; Hoerrner, R. S.; Javadi, G. J.; Cai, D.; Larsen, R. D. *Org. Lett.* **2003**, *5*, 4835. (d) Wang, J.-X.; McCubbin, J. A.; Jin, M.; Laufer, R. S.; Mao, Y.; Crew, A. P.; Mulvihill, M. J.; Snieckus, V. *Org. Lett.* **2008**, *10*, 2923 and references cited therein.

(8) Okazawa, T.; Satoh, T.; Miura, M.; Nomura, M. *J. Am. Chem. Soc.* **2002**, *124*, 5286.

(9) Campo, M. A.; Huang, Q.; Yao, T.; Tian, Q.; Larock, R. C. *J. Am. Chem. Soc.* **2003**, *125*, 11506.

(10) Capito, E.; Brown, J. M.; Ricci, A. *Chem. Commun.* **2005**, 1854.

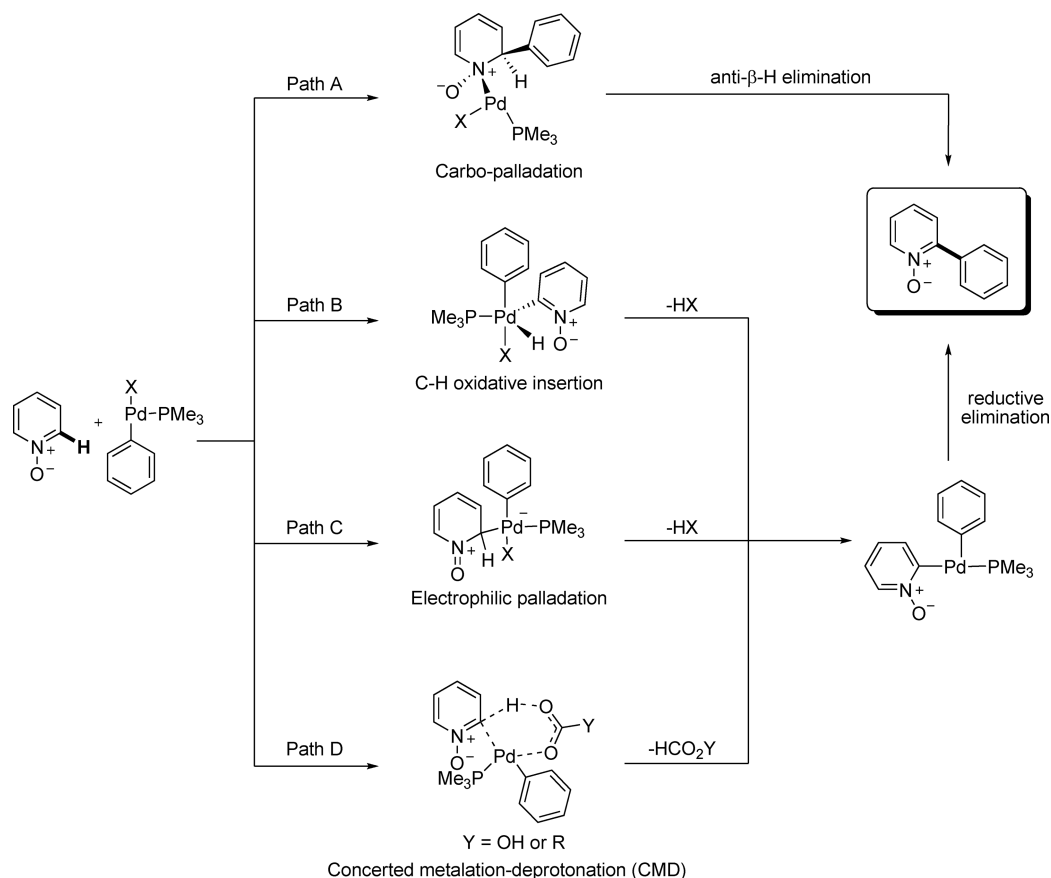
(11) Gorelsky, S. I.; Lapointe, D.; Fagnou, K. *J. Am. Chem. Soc.* **2008**, *130*, 10848.

(12) Zhao, X.; Yeung, C. S.; Dong, V. M. *J. Am. Chem. Soc.* **2010**, *132*, 5837.

(13) Davies, D. L.; Donald, S. M. A.; Macgregor, S. A. *J. Am. Chem. Soc.* **2005**, *127*, 13754.

(14) Biswas, B.; Sugimoto, M.; Sakaki, S. *Organometallics* **2000**, *19*, 3895.

SCHEME 2. The Four Possible Mechanisms of Direct Arylation

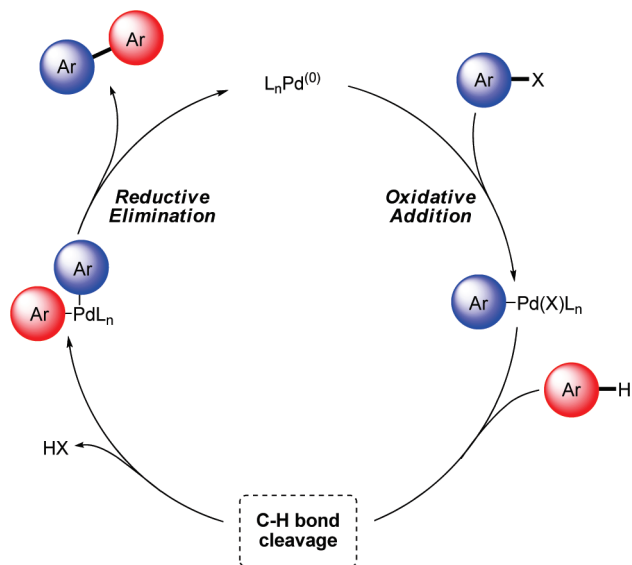


desired biaryl product and regenerates the active Pd⁽⁰⁾ catalyst. With the goal of obtaining a more detailed understanding of the catalytic cycle, and more specifically the intimate role of each of the primary reaction components, the order for each reagent in the coupling of 4-nitropyridine *N*-oxide and 5-bromo-*m*-xylene was obtained.¹⁵ Using either Pd(OAc)₂ and tri-*tert*-butylphosphonium tetrafluoroborate salt or Pd(P^{*t*}Bu)₃)₂ as the catalyst, the concentration of each reaction component was varied and the progression of the reaction at 110 °C was monitored. The initial time (*t*₀) of each kinetic run corresponded to the time at which the reaction flask was placed into the oil bath, which was preheated to 110 °C. During the course of the reaction, aliquots of the reaction mixture were removed, at which point the *N*-oxide readily precipitated from solution, thus stopping the reaction. The solvent was then removed and the resulting samples were analyzed by NMR spectroscopy for the formation of product with trimethoxybenzene as an internal standard.

There are several mechanistic scenarios to be considered for the direct arylation of pyridine *N*-oxides. One possible scenario involves oxidative addition as the rate-determining step of the reaction. In this case, one would expect to observe a first-order behavior in both aryl bromide and palladium catalyst, while zero-order behavior in pyridine *N*-oxide would be observed. If the C–H bond cleavage step were to be rate determining, two possible scenarios may be anticipated; if

the catalyst resting state is at the Pd⁽⁰⁾ species, then first-order behavior in the aryl halide, palladium catalyst, and the pyridine *N*-oxide may be expected. However, if the catalyst was saturated as a Pd^(II) species formed after oxidative addition, the aryl bromide would then be expected to exhibit zero-order behavior, while first-order behavior may still be

SCHEME 3. General Mechanism for the Palladium-Catalyzed Direct Arylation of Simple Arenes



(15) The choice of substrate was mainly guided for analytical simplicity as all analyses was done with ¹H NMR.

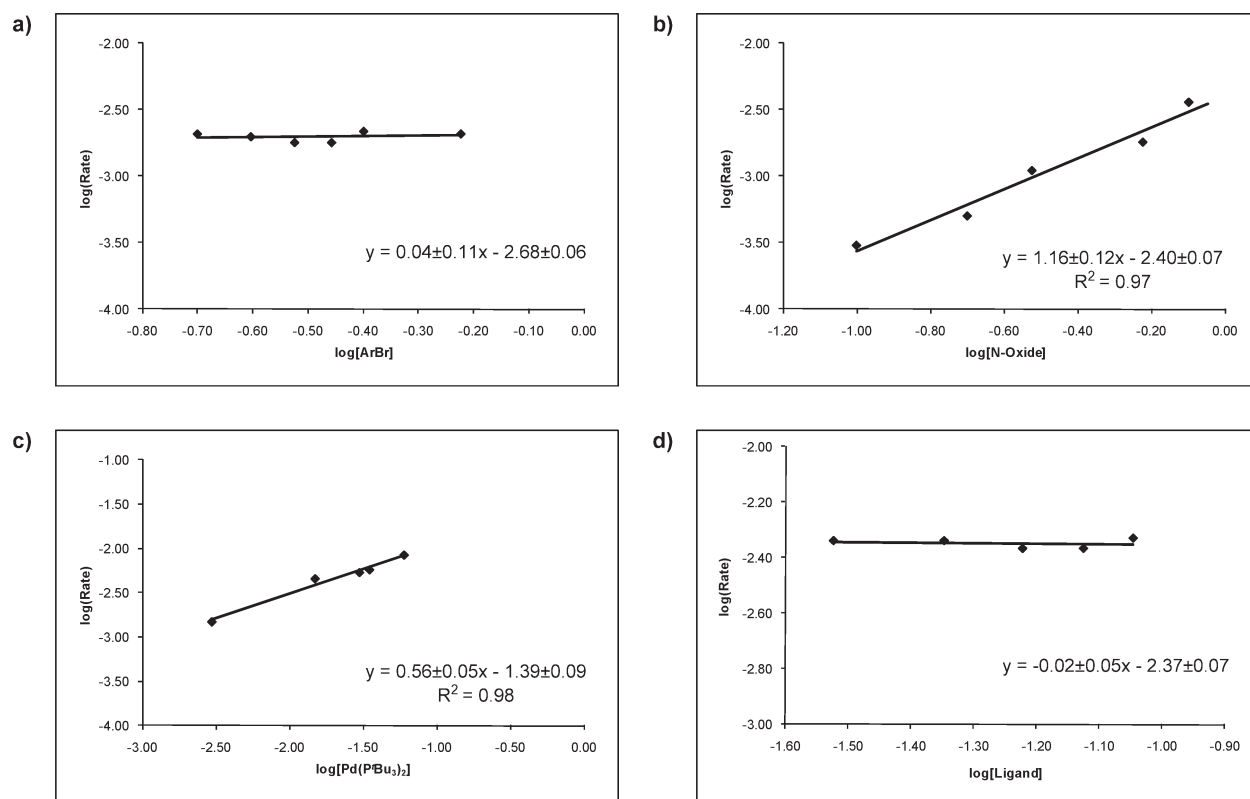


FIGURE 1. Log plot of the initial rate dependence on the concentration of (a) 5-bromo-*m*-xylene, (b) 4-nitropyridine *N*-oxide, (c) Pd(P'Bu₃)₂, and (d) P'Bu₃.

established for both the Pd catalyst and the *N*-oxide. The same observed kinetic consequences could be expected if reductive elimination was the rate-determining step, but these two cases may be distinguished by looking for the presence or absence of a significant kinetic isotope effect at the C2 position of the *N*-oxide (vide infra).

The order in 5-bromo-*m*-xylene was determined by plotting the log of the initial rate versus the log of the concentration, using 5 mol % of Pd(OAc)₂ as the precatalyst (Figure 1a). A slope of 0.04 was obtained revealing that varying the concentration of the aryl halide from 0.2 to 0.6 M has no effect on the reaction rate, thus establishing zero-order behavior in this system. The zero-order dependence in 5-bromo-*m*-xylene is indicative of a fast oxidative addition in which the palladium catalyst is saturated as a Pd^(II)-aryl species and thus ruling out the possibility of oxidative insertion being the rate-determining step.

The order in 4-nitropyridine *N*-oxide was also determined in a similar manner by varying its concentration from 0.1 to 0.8 M (Figure 1b). A slope of 1.16 was obtained indicating a first-order behavior in pyridine *N*-oxide. A first-order dependence on pyridine *N*-oxide suggests that a single molecule of the *N*-oxide participates at the transition state of the reaction, which is consistent with arene metalation or reductive elimination being the rate-determining step. Reductive elimination was discarded as a possible rate-determining step due to the observation of a significant kinetic isotope effect (KIE) in a side-by-side comparison of rates ($k_H/k_D = 3.3$) using pyridine *N*-oxide or pyridine *N*-oxide-*d*₅ as the starting azine.¹⁶

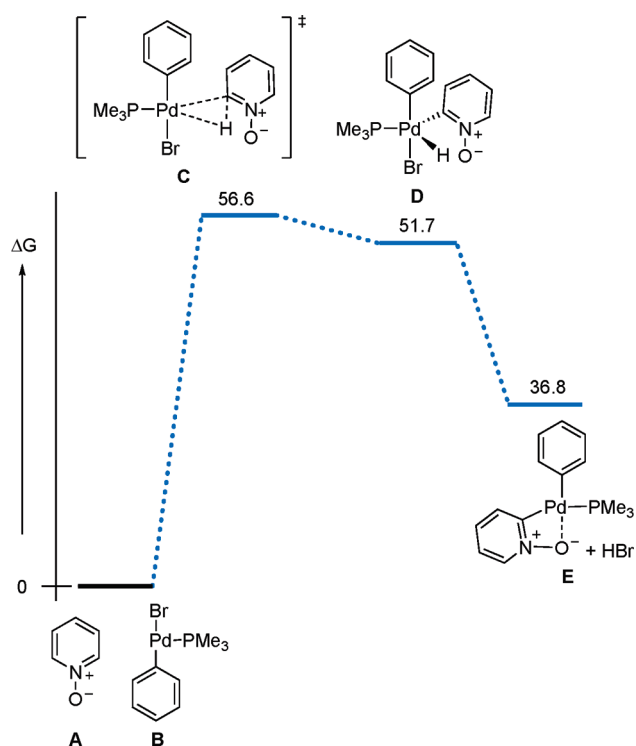
The rate-constant's dependence on catalyst concentration was determined by using Pd(P'Bu₃)₂ as the catalyst in order to eliminate catalyst preactivation. PivOH (30 mol %) was consequently added to account for the acetate that is normally in solution when Pd(OAc)₂ is used. The reaction rate was measured over a range of catalyst loadings of Pd(P'Bu₃)₂, varying from 1 mol % to 20 mol %. This order was determined with respect to an aryl bromide concentration of 0.3 M and an *N*-oxide concentration of 0.6 M, and a slope of 0.56 was obtained from the kinetic plot (Figure 1c), which is consistent with half-order behavior in catalyst. This behavior has been associated with systems in which the catalyst resting state is a dimer, while the active form of the catalyst is a monomer.¹⁷ According to the zero-order dependence on aryl bromide and first-order dependence on the *N*-oxide, the dimeric resting state should be found between the oxidative addition and arene metalation steps.

Finally, the order in ligand was determined, also using 5 mol % of Pd(P'Bu₃)₂ as the catalyst. No change in rate was observed over a range of ligand concentrations from a 1:2 Pd:ligand ratio to a 1:6 ratio (Figure 1d), thus establishing a zero-order behavior in this system. It has been previously determined that the oxidative addition product of Pd(P'Bu₃)₂ into the C–Br bond of an aryl bromide is a T-shaped complex bearing a single phosphine ligand and a free coordination site,¹⁸

(16) For results from a one-pot KIE experiment, please see ref 4a.

(17) (a) Fairlie, D. P.; Bosnich, B. *Organometallics* **1988**, *7*, 946. (b) Van Strijdonck, G. F. P.; Boele, M. D. K.; Kamer, P. C. J.; de Vries, J. G.; van Leeuwen, P. W. N. M. *Eur. J. Inorg. Chem.* **1999**, 1073. (c) Kina, A.; Hiroshi, I.; Hayashi, T. *J. Am. Chem. Soc.* **2006**, *128*, 3904. (d) Collum, D. B.; McNeil, A. J.; Ramirez, A. *Angew. Chem., Int. Ed.* **2007**, *46*, 3002. (e) Shen, Z.; Dornan, P. K.; Khan, H. A.; Woo, T. K.; Dong, V. M. *J. Am. Chem. Soc.* **2009**, *131*, 1077.

SCHEME 4. Free Energy Diagram ($\Delta G^\ddagger_{298\text{K}}$, kcal·mol⁻¹ in toluene) for the Relevant Intermediates, Transition States, and Products in the Oxidative Insertion Pathway



and as such, the arene metalation transition state should have at most one bound phosphine ligand. Additionally, the zero-order dependence on phosphine ligand supports the arene metalation transition state containing a single phosphine ligand and hence it is unlikely that dissociation of P^tBu₃ from Pd occurs before the rate-determining step of the reaction.

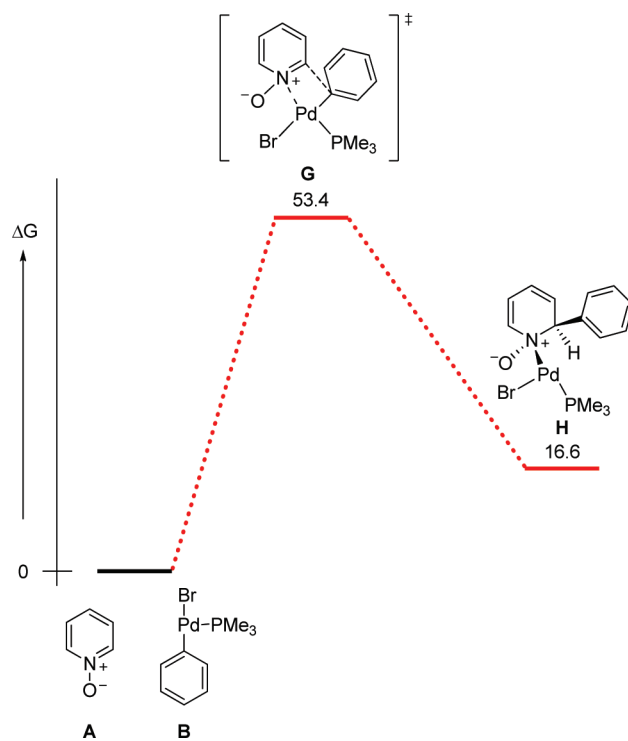
With a basic understanding of the catalytic cycle, the mechanism of the C–H bond cleavage was investigated in greater detail through both computational and experimental studies.

2. Computational Analysis. Quantum chemical¹⁹ density functional theory²⁰ calculations were used to assist in differentiating among the four possible mechanistic scenarios and determining the lowest energy pathway for the C–H bond cleavage step. All computations were performed at the Hybrid B3LYP level²¹ with a TZVP²² basis set for all atoms except palladium, for which a DZVP²³ basis set was used. The ligand (either PMe^tBu₂ or P^tBu₃) in the reaction was approximated with PMe₃ in all computations in order to reduce computational time. This is a commonly used technique^{3,5,11} and was not expected to change the qualitative findings of the calculations. Energy diagrams show the relative Gibbs Free Energies for the various transition states, intermediates, and products involved in each of the potential mechanisms. Calculations were performed in both the gas phase and with

a solvent correction for toluene.²⁴ The initial structures for all calculations are pyridine *N*-oxide (A) and a palladium(II) species (B, F, or F') coordinated by one PMe₃ ligand after oxidative insertion into the C–Br bond of bromobenzene. In the case of species F the bromide has been replaced by a bicarbonate anion while species F' contains an acetate anion in place of bromide. The relative geometry between the aryl group and the other anionic ligand is denoted as trans where the cis isomer is only marginally higher in energy.

Among the processes examined, the C–H oxidative insertion pathway (Scheme 4) was found to be the highest in energy, thus making it an unlikely candidate as the acting mechanism of the reaction. This pathway was found to proceed through transition state C having an energy of 56.6 kcal/mol and the resulting pentacoordinate Pd^(IV) intermediate D has an energy of 51.7 kcal/mol. Reductive elimination of HBr gives the common intermediate E having an energy of 36.8 kcal/mol. The Heck-type pathway (Scheme 5) is only slightly lower in energy than the C–H oxidative insertion pathway having a transition state (G) with an energy of 53.4 kcal/mol, though this results in an intermediate H with a relatively low lying energy of 16.6 kcal/mol.

SCHEME 5. Free Energy Diagram ($\Delta G^\ddagger_{298\text{K}}$, kcal·mol⁻¹ in toluene) for the Relevant Intermediates, Transition States, and Products in the Heck-Type Pathway



When investigating the CMD pathway two variants must be considered: an inner-sphere mechanism and an outer-sphere mechanism (Figure 2).^{3,5,11,25,26} An inner-sphere mechanism is characterized by an internal base coordinated to palladium participating in the CMD process. This base

(18) Stambuli, J. P.; Bühl, M.; Hartwig, J. F. *J. Am. Chem. Soc.* **2002**, *124*, 9346.

(19) Ziegler, T.; Autschbach, J. *Chem. Rev.* **2005**, *105*, 2695.

(20) (a) Hohenberg, P.; Kohn, W. *Phys. Rev. B* **1964**, *136*, 864. (b) Kohn, W.; Sham, L. J. *Phys. Rev. A* **1965**, *140*, 1133.

(21) Lee, C.; Yang, W.; Parr, R. G. *Phys. Rev. B* **1988**, *37*, 785.

(22) Schafer, A.; Huber, C.; Ahlrichs, R. *J. Chem. Phys.* **1994**, *100*, 5829.

(23) Godbout, N.; Salahub, D. R.; Andzelm, J.; Wimmer, E. *Can. J. Chem.* **1992**, *70*, 560.

(24) Foresman, J. B.; Keith, T. A.; Wiberg, K. B.; Snoonian, J.; Frisch, M. J. *J. Phys. Chem.* **1996**, *100*, 16098.

(25) Pascual, S.; de Mendoza, P.; Braga, A. A. C.; Maseras, F.; Echavarren, A. M. *Tetrahedron* **2008**, *64*, 6021.

(26) Lafrance, M.; Fagnou, K. *J. Am. Chem. Soc.* **2006**, *128*, 16496.

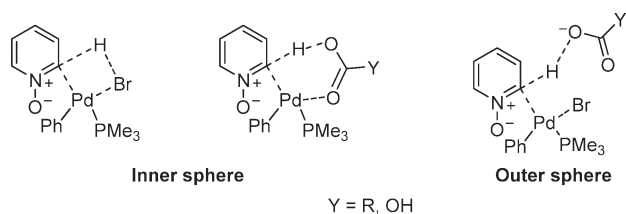
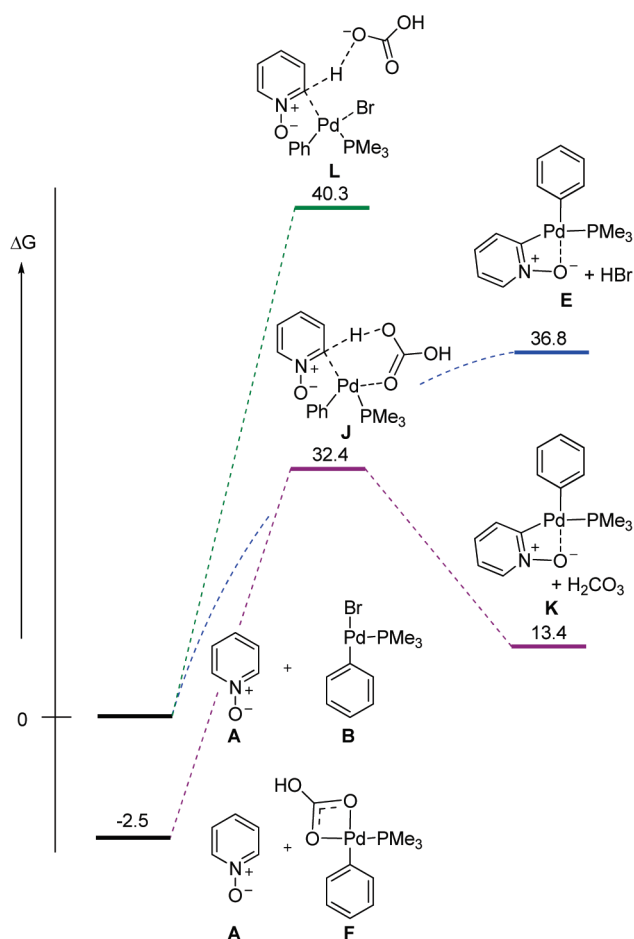


FIGURE 2. Inner- and outer-sphere mechanisms for the concerted metalation–deprotonation process.

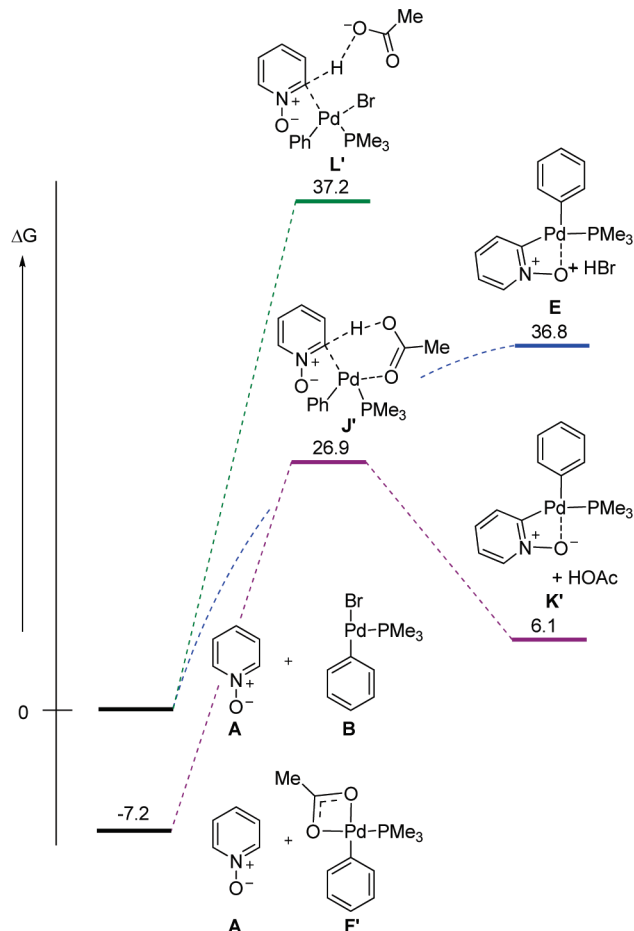
SCHEME 6. Free Energy Diagram ($\Delta G^{\ddagger}_{298\text{K}}$, kcal·mol⁻¹ in toluene) for the Relevant Intermediates, Transition States, and Products in the Inner- and Outer-Sphere CMD Pathways, Using Bicarbonate As the Base



can be either the halide from the aryl halide or a carbonate/carboxylate anion from a ligand exchange on palladium. Differentiated from this is the outer-sphere mechanism in which the deprotonation is performed by an external base (a carbonate or carboxylate anion).

Both CMD variants were found to be substantially lower in energy than the alternate pathways (Schemes 6 and 7). Starting with species **B** and bicarbonate as the external base, the outer-sphere mechanism had a transition state **L** energy of 40.3 kcal/mol and the inner-sphere mechanism starting from **F** as the Pd^(II) species had a transition state **J** energy of 32.4 kcal/mol. The inner-sphere mechanism with bromide as the base was found to have no thermodynamic barrier and arrives at the product **E** (36.8 kcal/mol) with subsequent loss

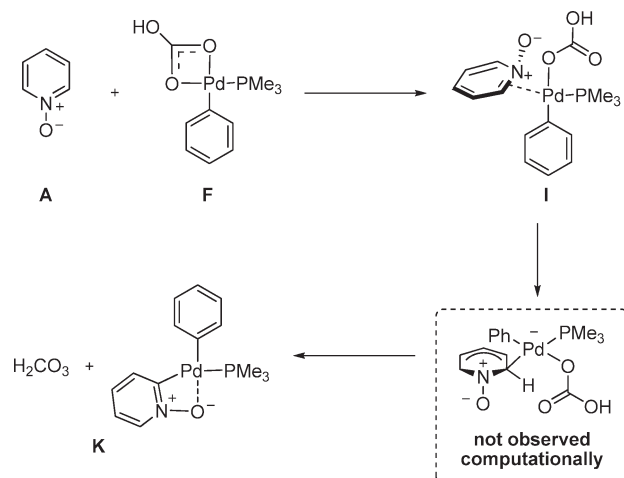
SCHEME 7. Free Energy Diagram ($\Delta G^{\ddagger}_{298\text{K}}$, kcal·mol⁻¹ in toluene) for the Relevant Intermediates, Transition States, and Products in the Inner- and Outer-Sphere CMD Pathways, Using Acetate As the Base



of HBr (Scheme 6). This pathway led to higher energy products than if bicarbonate was used as the base, and thus it was discarded. Calculations were also performed with acetate as the base. The relative energies of the transition states reflected those found when bicarbonate was used as the base, although the absolute values were found to be slightly lower (Scheme 7).

Efforts were made to locate the transition state energy leading to the Wheland intermediate in an S_EAr type pathway (Scheme 8) starting with **F** as the initial Pd^(II) species. However, only the intermediate **I** (18.9 kcal/mol), a η^2 π -complex having no cationic character on the aromatic ring, could be located. Departing from intermediate **I** this reaction pathway converges with that of the inner-sphere CMD pathway at transition state **J** (34.9 kcal/mol). Formation of the carbon–palladium bond and loss of H₂CO₃ yields products **K** (15.9 kcal/mol). The possibility of an S_EAr mechanism was thus discarded on the basis that no Wheland intermediate or complex containing arene cationic character could be located computationally.

From these results, the inner-sphere CMD mechanism was determined to be the most likely pathway for the C–H bond cleavage step in direct arylation. Computational results were also correlated to experimental findings to further support the proposal for a CMD mechanism. An Arrhenius plot was

SCHEME 8. Relevant Intermediates, Transition States, and Products in the S_EAr Pathway


constructed for the coupling between 4-nitropyridine *N*-oxide and 5-bromo-*m*-xylene (Figure 3) and the Arrhenius energy of activation was determined to be 18.5 kcal/mol. This value is in good agreement with the calculated ΔE^\ddagger of 17.6 kcal/mol (at 298 K, in toluene), suggesting that the inner-sphere CMD pathway is an energetically viable process.

The regioselectivity of the reaction was also examined and proved to be particularly illustrative. Computationally, the energies for arylation to take place at each position on the pyridine *N*-oxide ring were calculated for the inner- and outer-sphere mechanisms by using both carbonate and acetate as the base (Figure 4). In both cases, the inner-sphere mechanism was predicted to arylate preferentially at the C2 position, followed by C4 and with arylation at the C3 position being the highest in energy, while the outer-sphere mechanism was predicted to have the opposite selectivity, favoring arylation at the C4 position while arylation at the C2 position was the highest energy process. Pyridine *N*-oxide is known to be amphoteric acting as both a nucleophile and an electrophile.²⁷ The *N*-oxide moiety also imparts an increased acidity of the C–H bonds at positions 2 and 4 on the pyridine ring.²⁸ While our initial hypothesis was that an increased acidity of the C–H bond was a necessary component for the CMD mechanism, recent computational results from our group have shown that a more important factor is electropositive character at the position ortho to the nitrogen in the aromatic ring (as present at the C2 position of pyridine *N*-oxide).¹¹ Experimentally, the regiochemical outcome for the direct arylation of pyridine *N*-oxide is such that only arylation at the C2 position is observed, which is in agreement with calculated predictions for the inner-sphere mechanism.

The inner-sphere CMD mechanism also accurately predicts the site selectivity for substituted pyridine *N*-oxides (Table 1). When pyridine *N*-oxides bearing a phenyl or methylester substituent at the C3 position are used, the regioselectivity is sterically controlled and arylation takes place

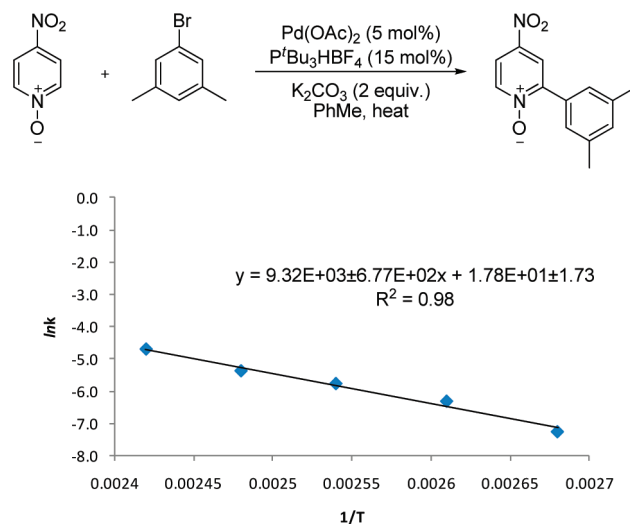


FIGURE 3. Arrhenius plot constructed for the coupling of 4-nitropyridine *N*-oxide.

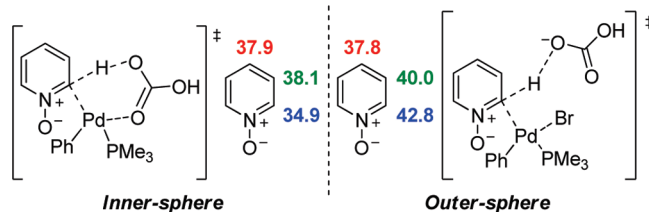
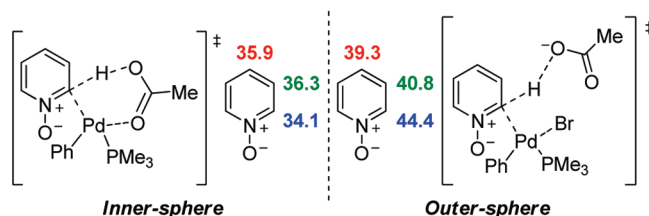
a) Using carbonate as the base

b) Using acetate as the base


FIGURE 4. Free energy of activation (ΔG^\ddagger_{298K} , kcal·mol⁻¹ in toluene) for the three possible sites of arylation via the inner- and outer-sphere mechanisms.

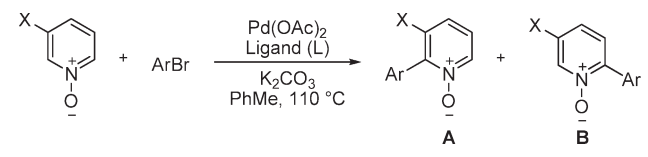
preferentially at the C6 position, suggesting that a steric bias for the less hindered site is controlling the regiochemical outcome of the reaction. A smaller C3 substituent, such as a methoxy group, results in nonselective arylation when P^tBu₃ is used as the ligand, which is in agreement with a steric argument for the selectivities observed, while selectivity for the C2 position is observed when the smaller P^tBu₂Me is used. This apparent ligand effect has been observed with other pyridine *N*-oxide and aryl halide substrates,^{4b,29,30} and along with the observed zero-order in ligand during kinetic experiments, it is also in agreement with the phosphine ligand being present on the metal at the CMD step.

(27) (a) Andersson, H.; Almqvist, F.; Olsson, R. *Org. Lett.* **2007**, *9*, 1335. (b) Taylor, E. C., Jr.; Crovetti, A. J. *Organic Syntheses*; Wiley: New York, 1963; Collect. Vol. IV, p 654; 1956; Vol. 36, p 53.

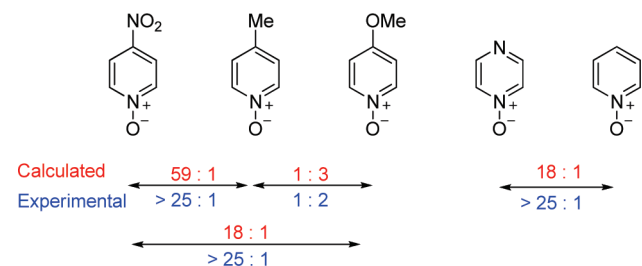
(28) (a) Paudler, W. W.; Humphrey, S. A. *J. Org. Chem.* **1970**, *35*, 3467. (b) Kreuger, S. A.; Paudler, W. W. *J. Org. Chem.* **1972**, *37*, 4188.

(29) Schipper, D. J.; El-Salfiti, M.; Whipp, C. J.; Fagnou, K. *Tetrahedron* **2009**, 4977.

(30) The regioselectivities for 3-fluoro- and 3-phenylpyridine *N*-oxide have also been reproduced stoichiometrically with **2**. See the Supporting Information.

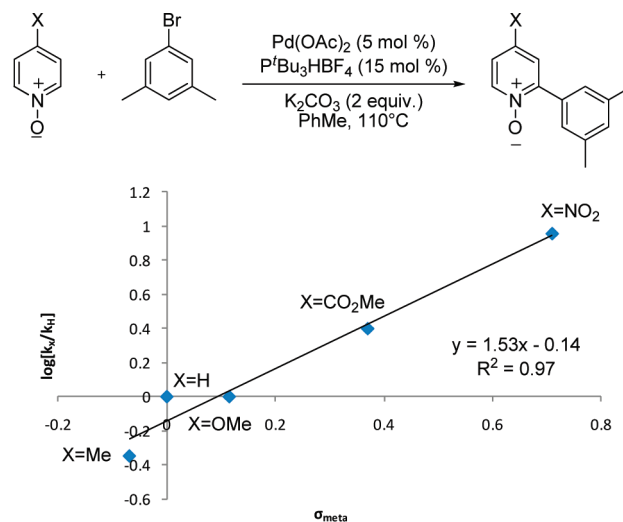
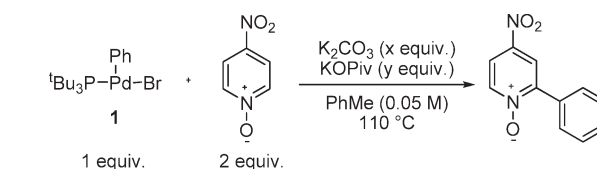
TABLE 1. Experimental and Computational Results for the Regioselectivity in the Direct Arylation of C3-Substituted Pyridine *N*-Oxides


entry	X =	calcd A:B (L = PMe ₃)	exptl A:B (L = P ^t Bu ₃)	exptl A:B (L = P ^t Bu ₂ Me)
1	Ph	1:11	1:10	
2	CO ₂ Me	1:4	1:7	
3	OMe	6:1	1:1	5:1
4	NO ₂	9:1	4:1	6:1
5	CN	4:1	10:1	15:1
6	F	76:1	25:1	

**FIGURE 5.** Computational and experimental results for competition experiments between pyridine *N*-oxides of different electronics.

In general, sterics seem to be the overriding factor in the observed selectivity. However, when smaller substituents are present subtle electronic factors come into play. This is exemplified by the inversed regioselectivity to the C2 position when a small C3 electron-withdrawing substituent, such as a nitro, cyano, or fluoro group, is present. The electron-withdrawing substituent could impart an electropositive character to the C2 position of the *N*-oxide through resonance and inductive effects, thus stabilizing the developing negative charge of the CMD transition state that involves the development of a negative charge at the C2 position. In all cases, the elaborated DFT model accurately predicts regiochemistry.

Additionally, one-pot competition experiments and computational predictions of relative rates under a CMD mechanism were performed (Figure 5) and it was found that the experimental values correlated well with the calculated ones. It was seen that in all cases, the aryl bromide reacted most readily with the more electron-deficient arene, which is contrary to what would be expected if S_EAr was the acting mechanism. The greater reaction rate of the methoxy-substituted *N*-oxide over the methyl-substituted *N*-oxide is due to the σ -withdrawing effect of the methoxy substituent to the meta position of the arene, which is also reflected in the positive σ_{meta} value of a methoxy substituent. The results of these competition experiments are also in agreement with the obtained Hammett plot, which provides a side-by-side comparison of the different *N*-oxides' reaction rates (Figure 6). In the past, Hammett studies conducted for direct arylation reactions have generally resulted in negative ρ values, and this observation was commonly used as the main argument in support of an S_EAr mechanism for direct arylation.² The obtained Hammett plot gives a ρ value of +1.53. The positive

**FIGURE 6.** Hammett plot for the direct arylation of C4-substituted pyridine *N*-oxides.**TABLE 2.** Yields of a Stoichiometric Reaction between 1 and 4-Nitropyridine *N*-Oxide, Using Different Bases

entry	K ₂ CO ₃	KOPiv	NMR Yield (%) ^a
1	none	none	0
2	10 equiv	none	5
3	none	10 equiv	29
4	10 equiv	10 equiv	31

^aTrimethoxybenzene as internal standard.

ρ value suggests the enhancement of rate with increasing electron-withdrawing ability of the substituent located at the C4 position of the *N*-oxide, which is in support of the CMD pathway. An electron-withdrawing substituent would be expected to stabilize the development of a negative charge at the CMD transition state, and thus lower the energy of the process.

3. Base Effects. Further experiments were performed to examine the nature of the base in the CMD process. The three-coordinate arylpalladium halide complex **1** (Table 2), a possible intermediate in the catalytic cycle, was synthesized according to a procedure reported by Hartwig et al.¹⁸ and was stoichiometrically reacted with 4-nitropyridine *N*-oxide in the presence of K₂CO₃ and/or KOiPr as a base. Reactivity was found to depend heavily on the presence of pivalate base in the reaction mixture. While no product is observed in the absence of any base, surprisingly low reactivity was observed when using K₂CO₃ (Table 2, entries 1 and 2). However, in the presence of pivalate, with or without K₂CO₃, the desired coupling product is obtained in approximately 30% yield (Table 2, entries 3 and 4).

The reaction rate was also found to depend heavily on the identity of the base present in the reaction mixture. Kinetic experiments were run with Pd(P^tBu₃)₂ as the catalyst in order to eliminate catalyst preactivation as a potentially significant

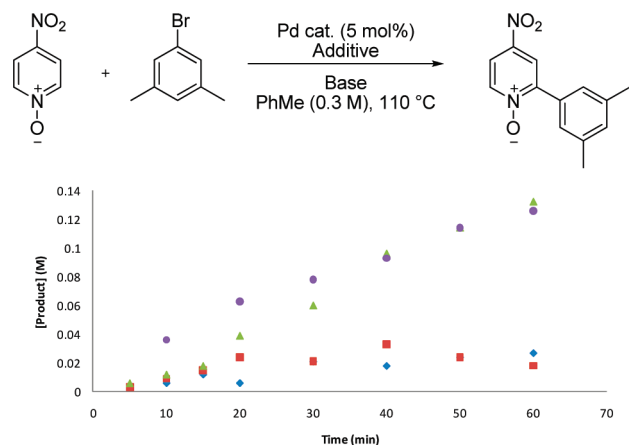


FIGURE 7. Dependence of rate on the identity of the base used. Conditions: (◆, light blue) Pd(P^tBu₃)₂, 2 equiv of K₂CO₃; (■, red) 5 mol % of Pd(P^tBu₃)₂, 2 equiv of KOPiv; (▲, green) Pd(P^tBu₃)₂, 2 equiv of K₂CO₃, 30 mol % of PivOH; and (●, dark blue) Pd(OAc)₂, 15 mol % of P^tBu₃·HBF₄, 2 equiv of K₂CO₃.

factor when measuring reaction rates. The rate of the reaction was observed to be slow when only one of K₂CO₃ or KOPiv was used, but when a combination of excess K₂CO₃ with a substoichiometric amount of PivOH was used, the reaction rate increased approximately 6-fold and was comparable to that of a reaction run under the standard reported conditions⁴ (Figure 7). The poor reactivity of a system using only KOPiv as the base may be attributed to the eventual buildup of PivOH in the reaction mixture, which could result in the proto-demetalation of a palladium aryl organometallic, generating reduced arene and catalytically inactive Pd^(II). This effect may also be the result of excess carboxylate saturating the catalyst and preventing its binding to the substrate. Using K₂CO₃ with a substoichiometric amount of PivOH would allow for the prevention of the buildup of acid by allowing the PivOH that is formed to be deprotonated by the K₂CO₃, thus regenerating the pivalate anion required for another turn of the catalytic cycle. When using Pd(OAc)₂ as the catalyst, however, no pivalate additive was required to achieve good reactivity, which alludes to a secondary role for Pd(OAc)₂.³¹ While Pd(OAc)₂ has always been considered to serve only as a precatalyst, these results are indicative of its ability to act as a source of soluble carboxylate base to perform the deprotonation at the CMD step.^{32,33}

To probe this hypothesis, the aryl palladium acetate complex **2** was synthesized³⁴ and reacted stoichiometrically with 4-nitropyridine *N*-oxide in the presence and absence of K₂CO₃. The conditions used were chosen to mimic the conditions used in the catalytic reaction. In both cases, the

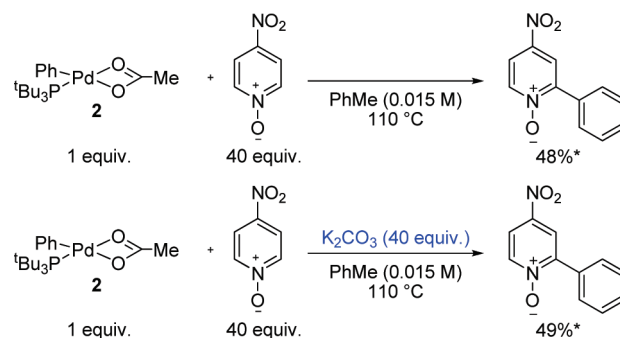
(31) While reactions having 10–30 mol % carboxylate have similar rates, it was noticed that when >40 mol % carboxylate is present under the standard conditions, a significant rate decrease is observed.

(32) To test this hypothesis, the rate of a reaction using a catalytic amount of KOAc was measured, but was found to be quite slow, likely due to the insolubility of KOAc in the toluene.

(33) When Pd(OPiv)₂ was used in place of Pd(OAc)₂ as the palladium precatalyst, an activation period of ca. 20 min was observed. Once the formation of product began, however, the rate of the reaction paralleled that of the reaction run with K₂CO₃ and catalytic PivOH. For kinetic experiments with Pd(OPiv)₂, see the Supporting Information.

(34) Barrios-Landeros, F. Oxidative Addition of Haloarenes by Pd(0) Complexes of Bulky Alkyl Phosphines: Synthesis of Intermediates and Mechanistic Studies, Dissertation, Yale University, 2007.

SCHEME 9. Stoichiometric Reactivity of Complex 2



*NMR Yields. Trimethoxybenzene used as internal standard.

obtained yields were identical, revealing little dependence of the stoichiometric reaction on the presence of K₂CO₃ (Scheme 9). The yields of these stoichiometric reactions are comparable to that of the analogous catalytic reaction.³⁵ These stoichiometric studies suggest that **2** is a likely intermediate in the catalytic cycle. Furthermore, the observed identical yields between the reactions run with and without K₂CO₃ are in support of acetate, and not carbonate, performing the necessary deprotonation at the CMD step.

The participation of **2** in the catalytic cycle is further supported by its ability to act as a competent catalyst as well as by the similarity in initial rates between a reaction run with catalytic Pd(P^tBu₃)₂ with PivOH and one run with a catalytic amount of **2** (Figure 8). A catalytic amount of KOPiv (5 mol %) was added to the reaction run with **2** as the catalyst in order to mimic the ratio of Pd to carboxylate base that is present when Pd(OAc)₂ is used as the catalyst.

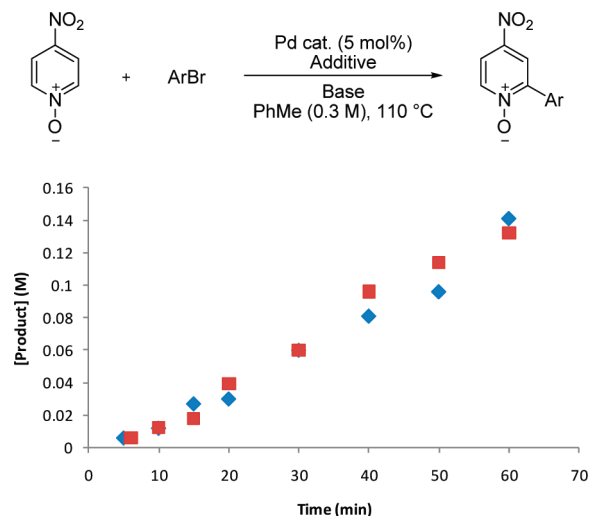
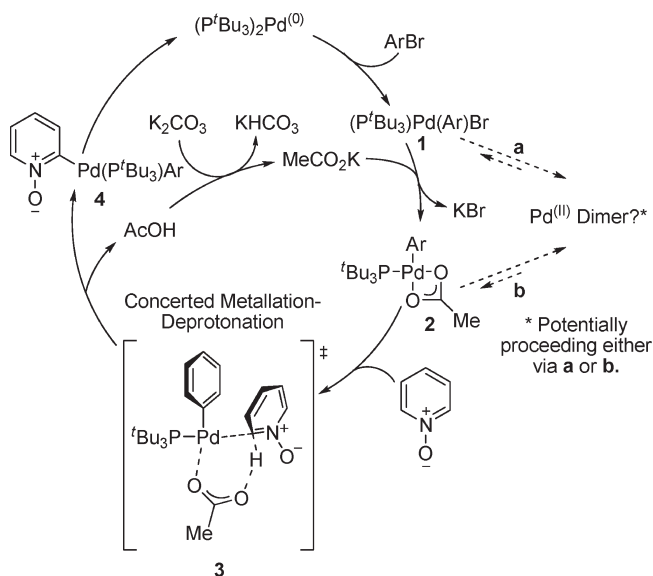


FIGURE 8. Initial rate of a reaction run with a catalytic amount of **2**. Conditions: (◆, blue) 1 equiv of bromobenzene, **2**, 2 equiv of K₂CO₃, 5 mol % of KOPiv; (■, red) 1 equiv of 5-bromo-*m*-xylene, Pd(P^tBu₃)₂, 2 equiv of K₂CO₃, 30 mol % of PivOH.

4. Summary of Mechanistic Data and Proposed Catalytic Cycle. Given the mechanistic insight we obtained from the results of the computational studies as well as the various

(35) Conditions: Bromobenzene (1 equiv), 4-nitropyridine *N*-oxide (2 equiv), Pd(OAc)₂ (5 mol%), P^tBu₃·HBF₄ (15 mol%), K₂CO₃ (2 equiv), PhMe, 110 °C, 16 h. NMR yield of 62%.

SCHEME 10. Proposed Catalytic Cycle for the Direct Arylation of Pyridine *N*-Oxides via a CMD Transition State

experiments performed, we are able to propose a revised catalytic cycle for the direct arylation of pyridine *N*-oxides (Scheme 10). The results from the kinetic experiments suggest a fast oxidative addition of the aryl halide into a Pd⁽⁰⁾ species after which the catalyst is saturated as a Pd^(II) species. According to the observed half-order dependence on catalyst concentration, this Pd^(II) species could possibly exist as an inactive dimer that is in equilibrium with the less favored active monomeric form of the catalyst.³⁶ Stoichiometric studies with different palladium complexes have pointed to the involvement of an acetate at the transition state as the deprotonating agent. The reaction likely proceeds via an κ^2 -bound acetate on the palladium metal **2** from which the pyridine *N*-oxide can displace one of the acetate oxygens and coordinate to the metal center.³⁷ The reaction is then proposed to proceed through a 6-membered inner-sphere CMD transition state, generating the palladium biaryl species that goes on to the reductive elimination step to give product and regenerate the Pd⁽⁰⁾ catalyst. The acetic acid generated in this process is likely deprotonated by the carbonate base in the reaction mixture, which regenerates the acetate required for another turnover of the catalytic cycle.

Conclusion

In conclusion, we have examined through kinetic and computational analysis the mechanism of direct arylation

(36) Efforts to isolate and characterize the dimeric resting state of the catalyst were unfruitful. However, as both the Pd-Br (**1**) and Pd-OAc (**2**) are known to be monomeric, we suspect the involvement of pyridine *N*-oxide in the dimeric form.

(37) It is likely that the initial coordination of pyridine *N*-oxide occurs via oxygen; for references on O-bound Pd complexes, see: Cho, S. H.; Hwang, S. J.; Chang, S. J. *Am. Chem. Soc.* **2008**, *130*, 9254.

of pyridine *N*-oxides. The data obtained from these studies allowed for the proposal of a revised catalytic cycle, which points to CMD being the rate-limiting step in the process. The critical role of the base in the CMD process was investigated in further detail in both catalytic and stoichiometric variations of the transformation. The observed dependence of reactivity on the presence of soluble carboxylate indicates that the acetate from the Pd(OAc)₂ precatalyst is acting as the deprotonating agent at the CMD step. This observation is also in accord with the prevalence of Pd(OAc)₂ being used as a precatalyst in direct arylation reactions and should be considered in the development of new direct arylation processes.

Experimental Section

General Procedure for the Direct Arylation of Pyridine *N*-Oxides with Aryl Bromides. Pyridine *N*-oxide (3 equiv), K₂CO₃ (2 equiv) P^tBu₃·HBF₄ (6–15 mol %), and Pd(OAc)₂ (5 mol %) were weighed into a round-bottomed flask equipped with a Teflon stir bar. The flask was fitted with a reflux condenser and the reaction vessel was then evacuated and refilled with argon (repeat 3 times). A solution of 5-bromo-*m*-xylene (1 equiv) in toluene (0.3 M with respect to aryl bromide) was purged with argon (10–15 min) and added to the reaction flask. The flask was placed in an oil bath and heated to 110 °C with constant stirring. The reaction was allowed to heat at 110 °C overnight after which the flask was removed from the oil bath and allowed to cool to room temperature. The reaction was then filtered through Celite (washing with CH₂Cl₂) and the filtrate was concentrated under reduced pressure then loaded onto a short silica gel column for chromatography.

2-(3,5-Dimethylphenyl)-4-nitropyridine *N*-oxide: ¹H NMR (400 MHz, CDCl₃, 293 K) δ 8.36 (1H, d, *J* = 7.2 Hz), 8.26 (1H, d, *J* = 3.2 Hz), 8.02 (1H, dd, *J* = 3.2, 7.2 Hz), 7.39 (2H, s), 7.16 (1H, s), 2.40 (6H, s); ¹³C NMR (100 MHz, CDCl₃, 293 K) δ 150.8, 142.0, 141.3, 138.4, 132.5, 130.6, 126.7, 121.6, 118.3, 21.4; HRMS calcd for C₁₃H₁₂N₂O₃ (M⁺) 244.0848, found 244.0846; IR (ν_{max}/cm⁻¹) 3106, 3085, 3055, 2917, 2859, 1520, 1341, 1278; mp 174–175 °C.

Acknowledgment. This paper is dedicated in memory of Keith Fagnou. H.-Y.S. thanks the Canadian Government for a PGS-M scholarship. L.-C.C. and D.R.S. thank the Canadian Government for PGS-D scholarships. This research was funded in part by NSERC, the Research Corporation (Cottrell Scholar Award; K.F.), the Ontario government (Premier's Research Excellence Award, K.F.), and the University of Ottawa. We thank Tom K. Woo for computing facilities use funded by the CFI and the ORF. The authors also thank Prof. John F. Hartwig and Prof. Melanie S. Sanford for helpful discussions during the preparation of this paper.

Supporting Information Available: Detailed experimental procedures for kinetics as well as results of DFT calculations. This material is available free of charge via the Internet at <http://pubs.acs.org>.